MDPI

Article

Shortwave UV Blue Luminescence of Some Minerals and Gems Due to Titanate Groups

Maxence Vigier, Emmanuel Fritsch *, Théo Cavignac, Camille Latouche and Stéphane Jobic

IMN, Institut des Matériaux de Nantes Jean Rouxel, Centre National de la Recherche Scientifique, Nantes Université, F-44000 Nantes, France
* Correspondence: emmanuel.fritsch@cnrs-imn.fr

Abstract: This article reviews blue shortwave-excited luminescence (BSL) in natural minerals and synthetic materials. It also describes in detail the emission of seven minerals and gems displaying BSL, as well as three references in which BSL is caused by titanate groups (TiO_6): benitoite, Ti-doped synthetic sapphire and spinel. Emission (under 254 nm shortwave excitation) and excitation spectra are provided, and fluorescence decay times are measured. It is proposed that BSL in beryl (morganite), dumortierite, hydrozincite, pezzotaite, tourmaline (elbaite), some silicates glasses, and synthetic opals is due to titanate groups present at a concentration of 20 ppmw Ti or above. They all share a broad emission with a maximum between 420 and 480 nm (2.95 to 2.58 eV) (thus perceived as blue), and an excitation spectrum peaking in the short-wave range, between 230 and 290 nm (5.39 to 4.27 eV). Furthermore, their luminescence decay time is about 20 microseconds (from 2 to 40). These three parameters are consistent with a titanate emission, and to our knowledge, no other activator.

Keywords: luminescence; titanate; beryl; pezzotaite; tourmaline; synthetic opal; lead glass; hydrozincite; dumortierite

1. Introduction

The purpose of this study is to propose an interpretation for lesser-known blue short-wave ultraviolet luminescence (BSL) observed in natural and synthetic minerals and gems. We consider a luminescence blue if the emission is perceived as blue. If one takes into account the mechanism of human color vision, this comprises emissions with maxima stretching from near-UV to about 500 nm, provided they are relatively wide (full width at half maximum –FWHM- of about 100 nm/0.65 eV). Shortwave ultra violet (SWUV or simply SW) radiation is usually defined as 254 nm (4.88 eV), as in standard UV lamps. Here, we extend that to a somewhat larger spectral range, to take into account the various values chosen by authors in the literature, ranging from about 240 to 300 nm (2.58 to 2.95 eV). However, for the experimental section, we used strictly 254 nm excitation. Only shortwave luminescence is required here, but blue longwave luminescence is not excluded as in anatase TiO_2 [1].

SWUV excited photoluminescence (SWPL) used in this work is distinct from excitation with a beam of electrons (cathodoluminescence–CL) which also produces blue luminescence in many minerals, and this may cause confusion. CL can be described as an irradiation experiment, creating defects as they are probed. Samples often heat, and sometimes change color. This does not happen with SWPL. CL uses particles with mass and charge, not SWPL. Also, because of generally high electron energy, and broad-band excitation, CL may use multiple excitation paths, with different emissions being prompted [2]. This may result in coupling with different defect states in the material. These states would not be probed with the comparatively narrow-band, lower energy SWPL. Also, CL probes strictly the surface (limited penetration of electrons) whereas SWPL tests the bulk of the material (see Figure 1).

One example is surface hydroxyl groups, that, although induced by SWUV exposure, are detected by blue Cl, not SWPL [3]. In jadeite, blue CL is attributed to Na^+ or Al^{3+} defect centers, whereas there is no blue SWPL of jadeite [4]. In summary, SWPL and CL are not identical but more complementary, emissions being induced by one (CL for example), being often not detected with the other, in particular surface- or oxygen-related defects.

Figure 1. Photo under daylight and under shortwave UV (254 nm) of the ten representative samples of BSL phenomena. (Photo: Maxence Vigier).

We aim to demonstrate that BSL is in many cases related to the presence of titanate groups, even if other, sometimes very different interpretations have been proposed. We sought BSL across a large number of species, not taking into account at first their structural or chemical characteristics. We then documented emission, excitation and time decay for those samples satisfying our criteria. We complemented this approach by an extensive bibliographical search for BSL across the chemical, mineralogical and gemmological literature.

BSL has previously been attributed to a number of activators. Our attention turned first to closed-shell compounds, that is complexes of transition elements without d electrons surrounded by oxygen atoms [5]. This family includes titanates, but also permanganates, chromates, vanadates, as well as molybdates, niobates, zirconates, tungstates and tantalates. Blasse (1980) has summarized their luminescence behavior. From this vast number of possibilities, we are interested in those absorbing around 4.8 eV (254 nm) and emitting light perceived as blue A well-studied, but rather unique example is scheelite ($CaWO_4$) where the BSL is ascribed to tungstate (WO_6) groups [6–8]. The only other closed shell compounds with similar constraints would be octahedral TiO_6 (again, [5]). This is confirmed by the study of benitoite by Gaft (2004), which proposes a detailed energy level scheme responsible for the emission of the titanate group in this titanate-containing mineral [9]. The relatively long decay time (2.6 µs) is explained by the presence of a forbidden state acting as a trap level.

BSL is also noted in rare-earth containing solids, with activators such as Ce^{3+} in apatite ($Ca_5(PO_4)_3(Cl,F,OH)$) [10]. More rarely, luminescence can also be attributed to rarer

elements or ions: UO^{2+} in turquoise ($CuAl_6(PO_4)_4(OH)_8 \cdot 4H_2O$) [11], Pb^{2+} in hydrozincite ($Zn_5(CO_3)_2(OH)_6$) [12], Tl+ in pezzotaite ($Cs(Be_2Li)Al_2Si_6O_{18}$) [13], or sulphur-doped $(S_2)^-$ in doped sodalite ($Na_8Al_6Si_6O_{24}Cl_2$) [14].

BSL is most frequently related to the presence of titanium, according to literature. Yet often details of the luminescence are missing (proof of Ti presence, excitation spectra or decay time measurements). In addition, the presence of isolated Ti^{3+} (*d-d* transitions) was assumed as a source of luminescence in several oxides like ZrO_2 or Al_2O_3 [15–17]. Recent theoretical modeling refutes this hypothesis in ZrO_2 and ascribes it to Ti^{4+} [18]. Minerals and gems containing Ti^{4+} cation in their nominal chemical formula are also known to present BSL phenomena. The best known example is benitoite ($BaTiSi_3O_9$), mentioned above, [9,19] and to a lesser degree baratovite ($KCa_7(Ti,Zr)_2Li_3Si_{12}O_{36}F_2$) and katayamalite ($KLi_3Ca_7Ti_2(SiO_3)_{12}(OH)_2$) [16].

Other authors have mentioned F-center as luminescence activators for BSL. In oxides and silicates, these are oxygen vacancies filled with two electrons, also noted "V^x_O" in Kröger–Vink notation. Examples include spinel ($MgAl_2O_4$) [20–22] and corundum (Al_2O_3) [23,24]. Some authors have attributed the pair formed by a F-centers and Ti^{4+} as the activator in Al_2O_3 [25], rutile (TiO_2) [26], hackmanite ($Na_8Al_6Si_6O_{24}(Cl_2,S)$) [27], and aluminosilicate glasses [28]. Each of these activators display a unique combination of emission/excitation/lifetime decay characteristics that makes it possible to pin down the origin of luminescence.

In the course of examining the luminescence of hundreds of minerals and gems, we have encountered a small number of BSL, which are considered unusual, sometimes not even described in articles, textbooks or websites. They seem to share comparable properties, mostly that the blue emission color and emission spectra are similar. Among those, BSL was observed in dumortierite ($Al_7BO_3(SiO_4)_3O_3$), synthetic spinel ($MgAl_2O_4$), synthetic opal and some rare tourmalines (dravite or elbaite, $NaMg_3Al_6(BO_3)_3Si_6O_{18}(OH)_4$/$Na(Li,Al)_3Al_6(OH)_4(BO_3)_3$.

Many titanium-containing minerals are known to have blue-to-blue-green shortwave-excited luminescence. Table 1 provides a summary of those minerals. The presence of titanium as chemical component, generally as a well-defined octahedral titanate group, makes these compounds the materials of choice as reference for the luminescence properties of the titanate group.

Table 1. Summary of luminescent properties of Ti-bearing natural minerals for which BSL has been documented. For all, the perceived luminescence color is blue and the purported is TiO_6.

Minerals	Emission nm (FWHM eV)	Excitation nm (FWHM eV)	Lifetime Decay	Reference
Baratovite $KCa_7(Ti,Zr)_2Li_3Si_{12}O_{36}F_2$	406 (1.00)	250 (1.63)	–	[16]
Benitoite $BaTiSi_3O_9$	420 (0.57)	240 (1.77) and 280 (1.29)	2.6 µs	[9]
Berezanskite $Ti_2\square_2KLi_3(Si_{12}O_{30})$	480	290	–	[29]
Katayamalite $KLi_3Ca_7Ti_2(SiO_3)_{12}(OH)_2$	406 (1.00)	250 (1.62)	–	[16]
Natisite $Na_2TiO[SiO_4]$	450 (0.94)	250 (1.00)	–	[29]
Penkvilksite $Na_4Ti_2Si_8O_{22} \cdot 4H_2O$	440 (0.99)	250 (1.00)	–	[29]

All of these minerals display a broad emission band centered between 406 and 450 nm (2.75 to 3.05 eV) with a 100 nm (0.65 eV) FWHM. In mineralogical studies, the excitation spectrum and lifetime decay associated with the luminescence maxima are not systematically measured (Table 1). Most BSL excitation spectra exhibits a large band about 50 nm (1 eV) FWMH in the 240–300 nm (4.13 to 5.16 eV) spectral range. The decay time is of the order of a µs. For natural minerals in Table 1, all BSL is linked to $[TiO_6]$ titanate groups.

It must be noticed that all the minerals in Table 1 do not contain iron. Other titanate containing minerals do contain iron as a major constituent and do not show BSL. Examples include non-luminescing ilmenite $FeTiO_3$, neptunite $KNa_2Li(Fe^{2+})_2Ti_2Si_8O_{24}$, warwickite $(Mg,Fe)_3Ti(O, BO_3)_2$, and titanomagnetite $Fe^{2+}(Fe^{3+}, Ti)_2O_4$. It is well-known that iron acts as a luminescence poison [27–29]. Often, the $O^{2-} \geq Fe^{3+}$ charge transfer participates in a well-known excitation-recombination process [30–33].

We also looked for evidence of BSL components in the material chemistry literature (Table 2). A small number of synthetic materials with titanate groups as a major constituent satisfy the conditions for BSL as well.

Table 2. Summary of luminescent properties of Ti-bearing synthetic compounds for which BSL has been documented. For all, the perceived luminescence color is blue.

Crystals	Emission nm	Excitation nm	Lifetime Decay	Proposed Cause	Reference
$LaMgS_{n-x}Ti_xO_8$	464–480	265		Ti^{4+}	[34]
Mg_2TiO_4	441	266			[35]
Na_2TiGeO_5	447	254		Ti^{4+}	[36]

The only FWHM available was 50 nm (0.74 eV) for the 254 nm excitation in $NaTiGeO_5$, comparable with that for natural minerals in Table 1.

After considering natural and synthetic materials containing titanate as a major component, and given the small number and relative rarity of some such compounds, we turned to materials that do not contain titanate as a component, but as an impurity (natural minerals and gems) or deliberate dopant (synthetic materials). In the synthetic compounds, titanium was mostly introduced in an effort to obtain luminescence (LED, emission and other scientific purposes). These materials are listed in Tables 3 and 4 with what is published of their luminescence properties.

Table 3. Summary of luminescent properties of natural compounds containing extrinsic Ti for which BSL has been documented. For all, the perceived luminescence color is blue.

Minerals	Emission nm (FWHM eV)	Excitation nm (FWHM eV)	Lifetime Decay	Proposed Cause	Reference
Aluminosilicate glass	490	270	0.7 and 5.6 µs	TiO_6	[28]
Bazirite $BaZrSi_3O_9$	460 (1.23)	250 (1.00)		Ti^{4+}	[37]
Diopside $CaMgSi_2O_6$	415 (1.53)	"Shortwaves"			[38]
Hydrozincite $Zn_5(CO_3)_2 (OH)_2$	430 (0.68)	240 (1.54)	0.7 µs	Pb^{2+}	[12]
Pezzotaite $CsAl_2Si_6O_{18}$	425 (0.84)	266	2–8.3 µs	Tl^+	[13]
Corundum: Sapphire Al_2O_3	425 (1.45)	250	42 µs		[39,40]
Spinel $MgAl_2O_4$	465 (0.88)	233 (1.64) and 260 (1.11)	3.5; 9.3; 46.3 µs	Ti^{4+} F-centers	[21]
Topaz $Al_2SiO_4(F,OH)_2$	460 (1.23)	320	"10^{-3}" ms	Heavy elements	[41]
Wadeite $K_2ZrSi_3O_9$	480 (1.13)	235 (1.14), 300 (0.69)		TiO_6	[29,42]

Table 4. Summary of luminescent properties of synthetic compounds containing extrinsic Ti for which BSL has been documented. For all, the perceived luminescence color is blue.

Crystals	Emission nm (FWHM eV)	Excitation nm (FWHM eV)	Lifetime Decay	Proposed Cause	Reference
Ti:BaZrO$_3$	408 (0.76)	274 (0.83)		Ti^{4+}	[43,44]
Ti:BaSnSi$_3$O$_9$	425 (0.70)	245 (1.04)		Ti^{4+}	[45]
Ti:CaZrO$_3$	427	260		Ti	[35]
Ti:Ca$_3$Al$_4$ZnO$_{10}$	370 (1.45)	265 (0.89)		Ti^{4+}	[36]
Ti:La$_2$Sn$_2$O$_7$	434	265		Ti	[35]
Ti:Lu$_2$O$_3$	380 (0.43)	240 (1.65)		Ti^{4+}	[46]
Ti:Mg$_5$SnB$_2$O$_{10}$	430 (1.42)	260 (1.12)		TiO$_6$	[47,48]
Ti:MgSnO$_4$	473	265	2.5 μs	Ti	[35]
ZrO$_2$ monoclinic	470	235, 290, and 375	2.46 μs	Ti^{4+}	[18,49]

Note that in Table 3 (natural minerals) titanium is the most often cited cause for BSL. Titanate groups are mentioned as the probable cause, but also Ti^{3+}, or the association of Ti with intrinsic defects. Finally, totally different causes are proposed for some, such as "heavy elements", with specific reference to Tl and Pb.

As expected, titanium is considered the activator in all the Ti-doped synthetic materials exhibiting BSL as it is the intended dopant used to trigger luminescence. There again, we note this element appearing as TiO$_6$ and Ti^{4+}.

Note that there are many more cases of blue luminescence attributed to titanium or titanate groups in the literature consulted (more than 25), but excitation data and/or proof of the presence of traces of Ti is missing in many compounds to establish that it is indeed BSL (see Table S1 in Supplementary Materials).

In addition to experimental work, recent advances in the theory of luminescence modelling in solids have proved useful to tackle the origin of luminescence when it is controversial. In particular, some attention has been paid to the role of titanium in oxides [18,44]. These studies confirmed without ambiguity that the blue luminescence in monoclinic ZrO$_2$ and BaTiZrO$_3$ is due to Ti^{4+} instead of F-centers.

On this bibliographic basis, it is apparent that titanate groups are likely to be the cause of BSL. We therefore proceeded with checking that the luminescence characteristics of BSL materials not described so far match those of the references materials selected or described in the literature. We actually started by checking that these compounds do contain traces of titanium.

2. Materials and Methods

We surveyed hundreds of gems and mineral specimens for BSL. Out of those, ten have been selected to represent either an adequate reference (benitoite, synthetic corundum, synthetic spinel) or as representative of BSL. They are listed in Table 5. They all fluoresce blue under shortwave UV (SWUV–254 nm, Figure 1). All samples were tested using Raman and other spectroscopic techniques to verify their nature. As hydrozincite is the only polycrystalline material, we assessed its detailed nature by X-ray diffraction. It contains a small amount of cerussite, which is not blue luminescing. All samples are part of the gemology teaching collection at Nantes University.

We include three references to be able to compare data obtained with the same instrument in the same conditions. This avoids variability factors (different lamps, correction or software) that may exist from one luminescence spectrometer to the other.

Table 5. Ten minerals or gem samples exhibiting BSL, selected for this study.

Minerals	Chemical Formula	Nature	Absorption Color	Sample
Benitoite	$BaTiSi_3O_9$	Natural	Blue	3684
Corundum: synthetic sapphire	Al_2O_3	Synthetic	Colorless	3697
Dumortierite	$Al_7BO_3Si_3O_{18}$	Natural	Blue	3977
Silicate glass: "Fondu du Jura"	65.7%w SiO_2, 9.1%w Na_2O, 25.2%w Al_2O_3	Synthetic	Blue	1846
Hydrozincite	$Zn_5(CO_3)_2(OH)_6$	Natural	White	4101
Beryl Morganite	$Be_3Al_2(SiO_3)_6$	Natural	Colorless	1865
Synthetic Opal	SiO_2, nH_2O	Synthetic	White with play of color	2029
Pezzotaite	$CsAl_2Si_6O_{18}$	Natural	Purple-Pink	966
Flame fusion synthetic Spinel	$MgAl_2O_4$	Synthetic	Colorless	1386
Tourmaline: Elbaite	$Na(Li,Al)_{1.5}Al_6(Si_6O_{18})(BO_3)_3(OH)_3$	Natural	Colorless	3056

The luminescence data were acquired with a Horiba JobinYvon Fluorolog-3 fluorimeter. The light source is a 450 W xenon lamp, the detector a Hamamatsu R13456 photo-multiplier. The emission spectra were carried out with an excitation at 254 nm, covering the range 300 to 900 nm with an excitation spectral bandwidth ("slit") of 4 nm and sampling every nanometer with an integration time of 1 s per point. The excitation spectra were acquired covering 240 to 400 nm with an emission spectral bandwidth ("slit") of 4 nm and sampling every nanometer with an integration time of 1 s per point. The acquisition was done via the Fluor-Essence software. The low-temperature luminescence experiments were performed in situ in a vacuum system with a conduction-cooling device at the temperature of liquid nitrogen (77 K) and with the same spectral parameters.

Fluorescence decay time is an important parameter to characterize the cause of luminescence. A fluorophore which is excited by a photon will drop to the ground state with a certain probability based on the decay rates through a number of different (radiative and/or nonradiative) decay pathways. To observe fluorescence, one of these pathways must be by spontaneous emission of a photon, for ex for BSL. BSL lifetime decay curves are fitted with Origin software with the following single exponential formula:

$$y = y0 + A1 * \exp\left(\frac{-(x - x0)}{t1}\right) \qquad (1)$$

where y0 is the y offset, A1 is the amplitude, x the time in seconds, x0 the x offset and t1 is the decay time measured.

Trace element data were obtained by laser ablation inductively coupled plasma mass spectrometry (LA-ICP-MS) using a G2 Excimer Laser Ablation System (at 50% of its maximum energy) coupled to a Varian quadrupole 820-MS system. Analyses consist for each sample of 5 lines of 60 spots. Each spot was obtained with an energy density of 4.54 J/cm^2 with a repetition rate of 10 Hz, spot size of 110 µm and a speed of 10 µm/s. The analysis consists of 30 s background acquisitions, 30 s data acquisition and 60 s time after each line (cell wash-out, gas stabilization, computer processing and move to next sample). We used two standard references: NIST 610 and NIST 612 measured at the beginning of the sequence and between each sample or two samples in a row [50]. The concentration of elements was calculated using the GLITTER software and calibrated using ^{27}Al [51].

3. Results

3.1. Inductively-Coupled Plasma Mass Spectrometry by Laser Ablation (LA-ICP-MS)

We investigated with LA-ICP-MS the elements that had been proposed as activators for BSL in the literature: chiefly Ti but also S, Tl and Pb. Results are reported in Table 6.

Table 6. Impurities concentrations (ppmw—parts per million weight) of the possible activators of BSL in the ten samples selected obtained by LA-ICP-MS techniques. avg (average), SD (standard deviation), nd (below limit of detection).

	Benitoite	Synthetic Sapphire	Dumortierite	Glass	Hydrozincite
	avg-SD	avg-SD	avg-SD	avg-SD	avg-SD
^{33}S	201.072–36.852	nd	1064.6–341.6	2136.8–624.5	10.1–1.0
^{47}Ti	Constituant	23.5–1.5	3658.2–127.2	1274.2–46.5	31.2–3.3
^{205}Tl	nd	nd	0.074–0.014	0.08–0.01	nd
^{208}Pb	0.354–0.021	1.3–0.1	11.6–0.9	2895.0–236.4	438.2–115.2
	Beryl (Morganite) avg-SD	Synthetic opal avg-SD	Pezzotaite avg-SD	synthetic spinel avg-SD	Tourmaline (Elbaite) avg-SD
^{33}S	703.216–225.848	254.6–36.5	396.3–131.5	nd	630.5–195.8
^{47}Ti	23.374–1.104	28.5–1.1	508.4–23.8	23.5–1.5	38.9–1.5
^{205}Tl	7.100–0.576	nd	2.59–0.14	nd	0.074–0.009
^{208}Pb	5.230–0.361	1.27–0.06	8.4–0.5	1.27–0.09	108.2–5.9

In all samples most of the activators proposed for blue luminescence are detected, but in contrasting amounts. Tl is detected in the ppm range or is below detection limits, making it a less likely candidate for BSL activation. Also, sulfur is not detected in one of the documented examples of BSL, synthetic sapphire. Pb is present in some samples but often at ppm level. On the other hand, titanium is always detected above the 20 ppm level in LA-ICP-MS on average, including in the reference materials. Nevertheless, extreme care must be taken when interpreting luminescence results based on a single criterion, in particular chemistry. Indeed, many emissions are caused by activators present only at the ppm level such Cr^{3+} in Ga_2O_3 [52] or the uranyl molecular ion in opal [53].

3.2. Photoluminescence Properties

3.2.1. Emission Spectra

Beyond the presence of the supposed activator, we must ascertain that all BSL described present similar spectroscopic characteristics for their emission. Figure 2 illustrates the emission spectra of our ten samples.

BSL is caused by an emission band with an apparent maximum between 414 and 463 nm (2.68 to 3.00 eV), as one would expect for a blue color perception. Also, the emission is always broad, ranging from about 75 to 100 nm (about 0.6 eV) FWHM. The emission is not always a single symmetrical band, so other contributions by other elements or maybe other electronic transitions could be part of this emission feature. In addition, the results are presented in nm for ease of comparison with other publications, but this induces a slight asymmetry of the spectral features. Nevertheless, overall, the emission of the new BSL materials have an emission profile which is close to that of the reference materials.

3.2.2. Excitation Spectra

Excitation spectra are critical to assign the cause of luminescence. They describe the absorptions responsible for the emission (Figure 3).
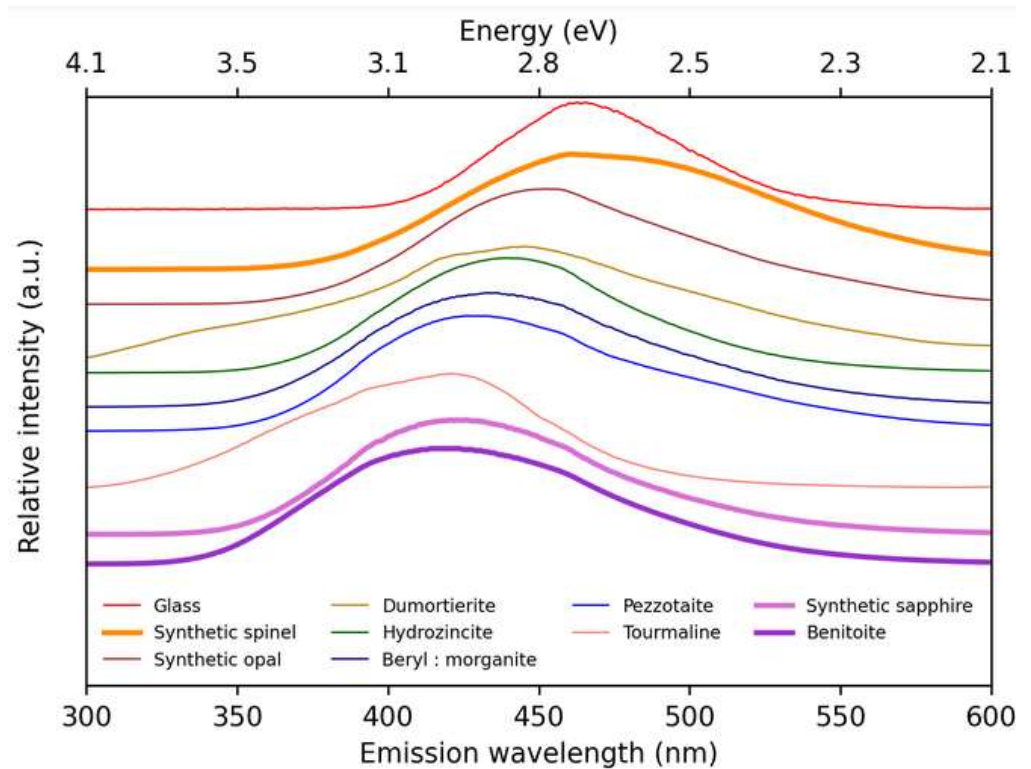
Figure 2. Emission spectra of our ten samples under λ_{ex} = 254 nm at room temperature. Apparent maxima of the broad emission band are located in the 414 to 463 nm range. Thicker lines mark reference materials. Spectra are shifted vertically for clarity.
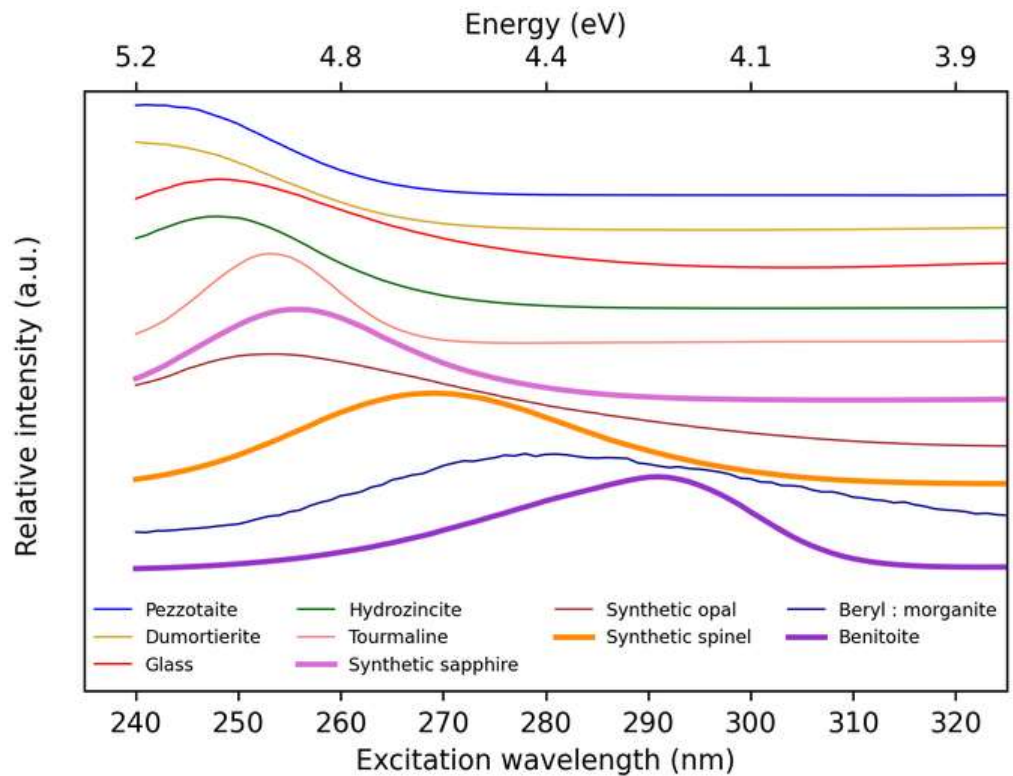

Figure 3. Excitation spectra of our ten samples for a luminescence excited by shortwave ultraviolet. Apparent maxima of the broad excitation band are located in the 240 to 290 nm range, as expected. Thicker lines mark reference materials. Spectra are shifted vertically for clarity.

Here also, the excitation spectral feature is not always a single symmetrical band. Two components seem present, one in the 240–250 nm (4.96–5.16 eV) range and the other in the 270–290 nm (4.27–4.59 eV) range. This is consistent with Gaft observations in several titanates that there are sometimes two excitation bands, one nearer 240 nm, and the other towards 290 nm [54]. These authors attribute the 240 nm excitation band to the allowed $^1A_{1g}$-$^1T_{2u}$ transition, and the weaker band at 290 nm to the formally forbidden $^1A_{1g}$-$^1T_{1u}$ transition. Nevertheless, overall, the excitation spectra of the reference and new BSL minerals are clearly comparable and consistent, if they are not identical.

3.2.3. Lifetime Decay of Luminescence

The third parameter to be taken into account when studying luminescence is the lifetime decay. Rarely studied in mineralogy, it is nevertheless essential to calculate it in order to determine which defect is at the origin of the luminescence. Similar activators should have similar lifetimes. The lifetime decay results of the ten BSL samples are presented in Figure 4.
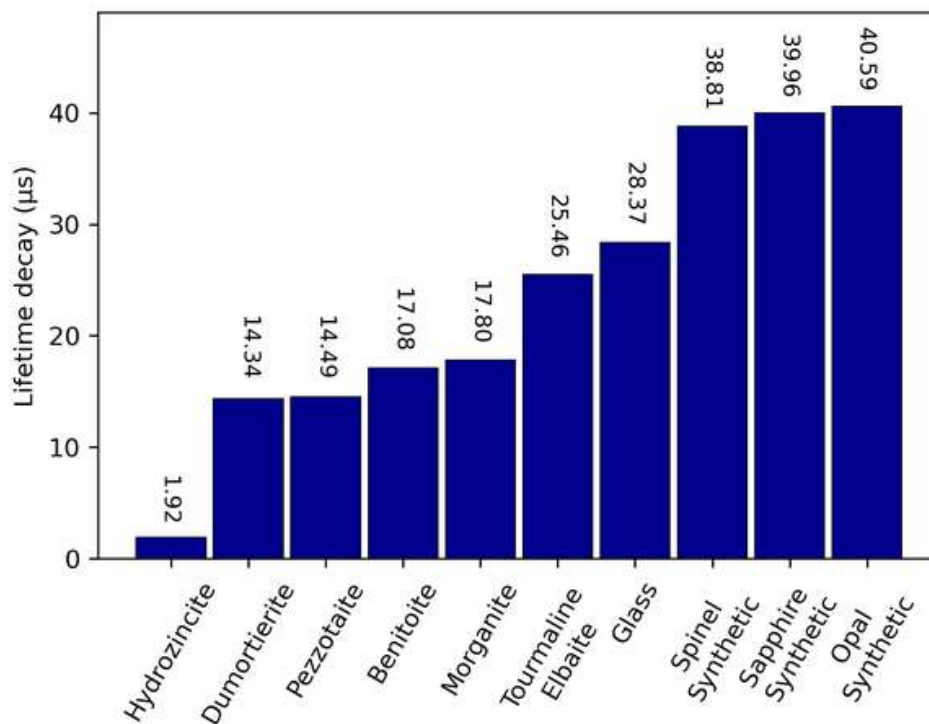

Figure 4. Lifetime decay of the ten samples showing BSL.

The values range from about 2 to approximately 40 μs on our instrument. The data for the reference materials are intercalated within the other new BSL, such as dumortierite, morganite, tourmaline and synthetic opal. Despite the apparent spread, this remains consistent for the same phenomenon across a wide variety of host atomic structures.

4. Discussion

All of the BSL minerals studied here show a broad emission band of about 100 nm FWHM wide (0.31 eV) between 414 and 463 nm (2.99 to 2.68 eV respectively) and a broad excitation band between 240 and 290 nm (4.27–5.16 eV) about 50 nm wide (0.89 eV), together with a decay lifetime of the order of 10–40 microseconds (Table 7). This data is consistent with titanate activator. We must first eliminate the other possible BSL activators invoked in the literature.

Table 7. Emission/excitation maxima of the ten samples showing BSL and associated lifetime decay.

Mineral	Emission Maxima (nm–eV)	Excitation Maxima (nm–eV)	Lifetime Decay (μs)
Benitoite	414–2.99	291–4.26	17.08
Corundum: Synthetic Sapphire	425–2.92	256–4.84	39.96
Dumortierite	446–2.78	Near 240–Near 5.16	14.34
Pb silicate glass	463–2.68	248–5.00	28.37
Hydrozincite	439–2.82	248–5.00	1.92
Beryl Morganite	433–2.86	278–4.46	17.8
Synthetic Opal	452–2.74	253–4.90	40.59
Pezzotaite	426–2.91	Near 240–Near 5.16	14.49
Flame fusion Synthetic Spinel	461–2.69	269–4.61	38.81
Tourmaline: Elbaite	420–2.95	253–4.90	25.46

The bibliographical search identifies four potential activators for the origin of BSL: titanium, lead, thallium or sulphur.

The luminescence of thallium in halogen compounds KCl, KBr, KI is close to that observed for BSL in terms of emission and excitation spectra [55]. However, Tl^+ lifetime is about 280 ns in KH_2PO_4, which is very different from our BSL values above 2 μs [56]. In addition, Tl is often below the limit of detection in BSL materials.

$(S_2)^-$ is very rarely mentioned as a source of blue luminescence in minerals [14], although it is rather known to be a common activator for emission in the orange-red spectral range [45,57,58]. There is little support for $(S_2)^-$ as activator as decay times are not provided and literature on this subject is scarce. Moreover, there is no relation between the S content that we measured and blue luminescence intensity.

Pb luminescence is mostly associated with emission in relatively longwave UV (mostly in 320–380 nm range) [54,59–63]. Also, Pb emission lifetimes appear to be much shorter than those observed in BSL, such as 190 to 300 ns at room temperature [55,64]. It also seems to be very dependent on Pb environment ranging from a few ns to microseconds in KCl, KBr [65]. It should be noted that some luminescence in the yellow range is attributed to Pb as in cerussite $(PbCO_3)$ or $SrTiO_3$ [66]. Thus, lead does not appear to be a source of the microsecond lifetime blue luminescence. In the specific case of our hydrozincite, it contains titanium, which is not the case of hydrozincite studied by [12] for which emission was attributed to Pb^{2+}. Furthermore, our sample contains a small amount of cerussite, which explains the high Pb concentration in ICPMS measurements, actually a contamination by a non-BSL phase.

Titanate groups are the most likely activators associated with BSL; it has the same position maxima and width in emission and excitation spectra and same order of magnitude of decay times (Table 7), as confirmed by running references in the same manner as the BSL "unknowns" have.

We demonstrated that titanate is at the origin of BSL in dumortierite, whose origin has always been supposed to be related to titanium, but no detailed literature is available on the subject [29]. Note that many pink or blue quartz, colored by varieties of dumortierite, show this luminescence. We were also able to see the BSL in a synthetic opal. This is more surprising as blue luminescence in natural opals and amorphous silica is known to be associated with the presence of non-bonding oxygen or oxygen deficiency in silica (ODC) tetrahedra [54,67,68]. However, the common blue luminescence of opals is mostly triggered in longwave (365 nm) in contrast to that caused by the presence of titanate which is SW-excited only. It is logical that synthetic opal offers different luminescence behavior having a slightly different structure [69]. It is possible that TiO_2 substitutes partially for ZrO_2 the material between SiO_2 sphere– in this synthetic opal [70].

We describe for the first time blue luminescence in beryl, in this case morganite. The similarity of the structure of beryl and pezzotaite makes it likely that BSL in the gems

would have similar causes. It is what we find and then, we ascribed its blue luminescence to TiO_6 center presence in both of them. Titanium probably substitutes for Al in its octahedral site in either mineral. This is a rare luminescence in beryl/pezzotaite as it necessitates the presence of traces of Ti and the virtual absence of iron. BSL is limited in beryl to near colorless to pink varieties (goshenite, morganite) and it is not found in more common, iron-containing beryl varieties.

It is not surprising that titanate is found in a wide variety of minerals. Titanium is the ninth most abundant constituent of the earth's crust and mantle [71]. Naturally, it can be found as a component of numerous minerals such as rutile/anatase/brookite (TiO_2), ilmenite ($FeTiO_3$), sphene ($CaTi(SiO_4)O$) and many others. However, titanium is present in the majority of soils, rocks and sediments in very small quantities (a few percent to ppm). In many natural crystalline compounds, Ti has two main valences, Ti^{3+} and Ti^{4+} and is mainly found in octahedral coordination [72]. It is rarely found as TiO_4/TiO_5 [73–75]. As with many transition elements, the mere presence of a few ppm is a potential source of unique physical, in this case optical, properties. For decades, titanium has been known to be a cause of luminescence under cathode rays, ultraviolet light, flame excitation or heating in many compounds, so it is a well-established and likely luminophore or activator [76].

Based on the work of Sidike et al. 2010 and Satoh et al. 2017, correlations have been observed between the Ti-O distance and the emission wavelength (Figure 5) [16,77]. However, very few studies determine directly the real Ti-O distance in Ti-doped compounds. The Ti-O distance mentioned in many publications is the metal-oxygen distance in the titanium-free compound. When present as an impurity, the determination of the exact (average) Ti-O distance would require using synchrotron techniques, for example. Nevertheless, we plotted the position of the emission versus estimated Ti-O bond length (Figure 5) using measured or estimated Ti-O bond lengths available in the literature.
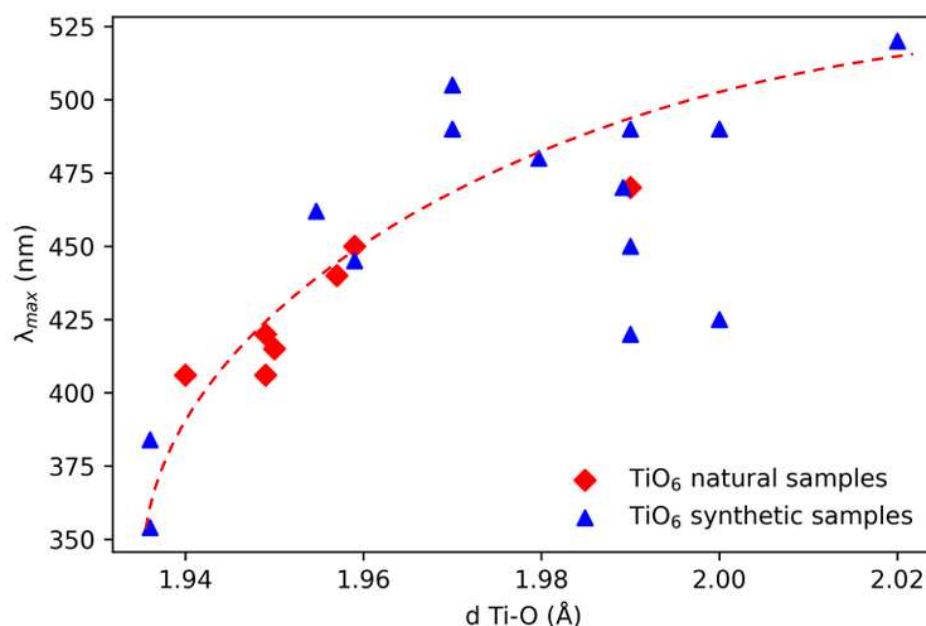

Figure 5. Position of the emission versus estimated Ti-O bond length in Ti-bearing compounds. Most of the Ti-O distances are estimated by structural analysis (DRX) or synchrotron. A visual guide, not a fit, in interrupted red indicates a trend. Data provided in SI.

A visual guide, not a fit, indicates a correlation trend between the length of the Ti-O distance and the luminescence emission maximum. Counter-examples are curiously located only in the 1.98 to 2.00 Å range. This means that emission is shifted from blue to green as Ti-O lengthens leading the blue-green, green, yellow luminescence due to titanate groups at longer Ti-O, superior to 2 Å although alternative possibilities have been proposed (see below).

Our assignment of BSL to the titanate group is based on four measurements. The coincidence for seven minerals (plus three references) is striking; yet it is always possible in luminescence studies that there is an alternate cause, due to a coincidence of spectral properties between two activators. Despite the difference in lifetime measurements, the resemblance between the blue emission of Pb^{2+} in hydrozincite (without titanium) and hydrozincite with titanium merits further investigation. To complete the present work, it would be interesting to probe further with time resolved luminescence, and also perform temperature studies.

The lack of information on the luminescence of minerals prevents us from mentioning further possible candidates for BSL. There are a number of articles regarding the luminescence of titanium-containing materials which indicate potential BSL, but often either the effective color or the excitation wavelengths are missing. Thus, the list of BSL materials might be much longer, but often only the emission data is provided, which does not stop many authors from interpreting the source of a simple blue luminescence as being due to titanates without chemical analyses proving the presence of Ti as a trace. Many blue-white luminescences are ascribed to TiO_6 in fluorescence database (such as Fluomin), for example murmanite $Na_4Ti_4(Si_2O_7)_2O_4\ 4H_2O$, a potential candidate if more information is provided. The visual description is clearly insufficient to identify BSL in hibonite $Ca_2(Al,Ti)_{24}O_{38}$ [78]. A non-exhaustive list of many luminescent compounds satisfying at least in part BSL criteria is provided in SI.

Titanate related luminescence is not restricted to BSL. Some minerals emit a green to a yellow luminescence with the same excitation spectrum and similar lifetimes to BSL. This is recorded for natural minerals such as andalusite [54], topaz [41], cassiterite [79] lorenzite, talc, uvarovite [29], baghdadite [16], chrysoberyl: alexandrite [54] and enstatites [80]. This is also true of several chemical compounds such as $MgSn_2O_4$, zirconium titanate doped with lanthanum or $BaTi(PO_4)_2$ [81–83] In some of these compounds, titanium is present in TiO_5 groups, which may explain the shift of color [84–86]. It has also been proposed that there is a link between the shift of the emission wavelength and the amount of titanium in the solid, (in stannates [34]). Finally, some authors mention the presence of oxygen vacancies in TiO_5 polyhedra as an explanation for emissions in the green to yellow range [35,87,88]. These activators have also been proposed for BSL, so yellow and green emissions may be induced by titanate groups with different environments from those leading to BSL.

5. Conclusions

We have demonstrated for the first time that BSL is due to octahedral titanate groups in seven natural minerals and synthetic materials: dumortierite, hydrozincite, beryl, pezzotaite, some elbaites, some lead aluminosilicate glasses and some synthetic opals. This was established by comparing the luminescence properties with reference materials for which the origin of BSL has been firmly established as being due to TiO_6. BSL minerals are characterized by a broad emission band in the spectral range perceived as blue, between 400 and 500 nm (3.1 to 2.48 eV), respectively. This band is relatively broad (about 100 nm–near 0.6 eV). It is excited between 250 and 300 nm, with an excitation band about 50 nm wide (0.6 eV). Finally, the decay lifetime is of the order of ten microseconds, spreading from 2 to 40 microseconds.

It is apparent from a literature search that many more minerals or materials might possess a titanate-induced BSL. Yet, because of the lack of details regarding luminescence parameters (excitation spectrum and decay time, for example) one cannot prove the titanate origin of these emissions (see Tables S1 and S2 in Supplementary Materials). In addition, recent progress in luminescence modelling has started to confirm titanate origin where the origin of BSL was ambiguous. There is reason to believe that, in the future, the titanate activation of BSL will be demonstrated for an increasing number of minerals (natural or synthetic).

Supplementary Materials: The following supporting information can be downloaded at: https: //www.mdpi.com/article/10.3390/min13010104/s1, Table S1: Mineral and synthetic compounds on which Ti-related blue luminescence (possibly BSL) has been described or inferred [1,27,29,39,79,83,88–101]. Table S2: Data associated with Figure 5, mineral & formula, Ti-O distance, emission maxima (in nm and eV), bibliographic sources for luminescence and Ti-O distance [1,9,16,29,40,77,89–92,102–119].

Author Contributions: Conceptualization, M.V.; Data curation, M.V.; Formal analysis, M.V.; Investigation, M.V. and C.L.; Methodology, M.V., E.F. and C.L.; Resources, E.F.; Supervision, E.F. and S.J.; Validation, E.F. and S.J.; Visualization, M.V., E.F., T.C., C.L. and S.J.; Writing–original draft, M.V., E.F. and C.L.; Writing–review and editing, M.V., E.F. All authors have read and agreed to the published version of the manuscript.

Data Availability Statement: Not applicable.

Conflicts of Interest: The authors declare no conflict of interest.

References

1. Tang, H.; Berger, H.; Schmid, P.E.; Lévy, F.; Burri, G. Photoluminescence in TiO_2 anatase single crystals. *Solid State Commun.* **1993**, *87*, 847–850. [CrossRef]
2. Marshall, D.J. *Cathodoluminescence of Geological Materials*; Unwin-Hyman: Boston, MA, USA, 1988; 146p.
3. Garcia-Guinea, J.; Garrido, F.; Lopez-Arce, P.; Correcher, V.; de la Figuera, J. Spectral Green cathodoluminescence emission from surfaces of insulators with metal-hydroxyl bonds. *J. Lumin.* **2017**, *190*, 128–135. [CrossRef]
4. Takahashi, N.; Tsujimori, K.; Kayam, M.; Nishido, H. Cathodoluminescence petrography of P-type jadeitites from the New Idria serpentinite body, California. *J. Mineral. Petrol. Sci.* **2017**, *112*, 291–299. [CrossRef]
5. Blasse, G. The Luminescence of Closed-Shell Transition-Metal Complexes. New Developments. In *Luminescence and Energy Transfer*; Springer: Berlin/Heidelberg, Germany, 1980; pp. 1–41.
6. Hemphill, W.R.; Tyson, R.M.; Theisen, A.F. Spectral luminescence properties of natural specimens in the scheelite-powellite series, and an assessment of their detectivity with an airborne Fraunhofer line discriminator. *Econ. Geol.* **1988**, *83*, 637–646. [CrossRef]
7. Tyson, R.M.; Hemphill, W.R.; Theisen, A.F. Effect of the W:Mo ratio on the shift of excitation and emission spectra in the scheelite-powellite series. *Am. Mineral.* **1988**, *73*, 1145–1154.
8. Bode, J.H.G.; Van Oosterhout, A.B. Defect luminescence of ordered perovskites A_2BWO_6. *J. Lumin.* **1975**, *10*, 237–242. [CrossRef]
9. Gaft, M.; Nagli, l.; Waychunas, G.; Weiss, D. The nature of blue luminescence from natural benitoite $BaTiSi_3O_9$. *Phys. Chem. Miner.* **2004**, *31*, 365–373. [CrossRef]
10. Waychunas, G.A. Apatite luminescence. *Rev. Mineral. Geochem.* **2002**, *48*, 701–742. [CrossRef]
11. Nikbakht, T.; Kakuee, O.; Lamehi-rachti, M. An efficient ionoluminescence analysis of turquoise gemstone as a weakly luminescent mineral. *Spectrochim. Acta Part A Mol. Biomol. Spectrosc.* **2017**, *179*, 171–177. [CrossRef]
12. Gaft, M.; Seigel, H.; Panczer, G.; Reisfeld, R. Laser-induced time-resolved luminescence spectroscopy of Pb^{2+} in minerals. *Eur. J. Mineral.* **2002**, *14*, 1041–1048. [CrossRef]
13. Panczer, G.; Gaft, M.; De Ligny, D.; Boudeulle, M.; Champagnon, B. Luminescent centres in pezzottaite, $CsBe_2LiAl_2Si_6O_{18}$. *Eur. J. Mineral.* **2010**, *22*, 605–612. [CrossRef]
14. Chang, I.F.; Onton, A. Optical properties of photochromatic sulfur-doped chlorosodalite. *J. Electron. Mater.* **1973**, *2*, 17–46. [CrossRef]
15. Carvalho, J.M.; Rodrigues, L.C.; Hölsä, J.; Lastusaari, M.; Nunes, L.A.; Felinto, M.C.; Brito, H.F. Influence of titanium and lutetium on the persistent luminescence of ZrO_2. *Opt. Mater. Express* **2012**, *2*, 331–340. [CrossRef]
16. Sidike, A.; Kobayashi, S.; Zhu, H.-J.; Kusachi, I.; Yamashita, N. Photoluminescence of baratovite and katayamalite. *Phys. Chem. Miner.* **2010**, *37*, 705–710. [CrossRef]
17. Lupei, A.; Lupei, V.; Ionescu, C.; Tang, H.G.; Chen, M.L. Spectroscopy of Ti^{3+}: α-Al_2O_3. *Opt. Commun.* **1986**, *59*, 36–38. [CrossRef]
18. Lafargue-dit-Hauret, W.; Schira, R.; Latouche, C.; Jobic, S. Theoretical calculations meet experiment to explain the luminescence properties and the presence of defects in m-ZrO_2. *Chem. Mater.* **2021**, *33*, 2984–2992. [CrossRef]
19. Takahashi, Y.; Kitamura, K.; Iyi, N.; Inoue, S.; Fujiwara, T. Blue photoluminescence of germania-stabilized benitoite. *J. Ceram. Soc. Jpn.* **2008**, *116*, 1143–1146. [CrossRef]
20. Pathak, N.; Ghosh, P.S.; Gupta, S.K.; Mukherjee, S.; Kadam, R.; Arya, A. An insight into the various defects-induced emission in $MgAl_2O_4$ and their tunability with phase behavior: Combined experimental and theoretical approach. *J. Phys. Chem. C* **2016**, *120*, 4016–4031. [CrossRef]

21. Sawai, S.; Uchino, T. Visible photoluminescence from $MgAl_2O_4$ spinel with cation disorder and oxygen vacancy. *J. Appl. Phys.* **2012**, *112*, 103523. [CrossRef]

22. Raj, S.S.; Gupta, S.K.; Grover, V.; Muthe, K.P.; Natarajan, V.; Tyagi, A.K. $MgAl_2O_4$ spinel: Synthesis, carbon incorporation and defect-induced luminescence. *J. Mol. Struct.* **2015**, *1089*, 81–85. [CrossRef]

23. Mikhailik, V.B.; Kraus, H.; Balcerzyk, M.; Czarnacki, W.; Moszynski, M.; Mykhaylyk, M.S.; Wahl, D. Low-temperature spectroscopic and scintillation characterisation of Ti-doped Al_2O_3. *Nucl. Instrum. Methods Phys. Res. Sect. A Accel. Spectrometers Detect. Assoc. Equip.* **2005**, *546*, 523–534. [CrossRef]

24. Chen, W.; Tang, H.; Shi, C.; Deng, J.; Shi, J.; Zhou, Y.; Yin, S. Investigation on the origin of the blue emission in titanium doped sapphire: Is F^+ color center the blue emission center ? *Appl. Phys. Lett.* **1995**, *67*, 317–319. [CrossRef]

25. Mikhailik, V.B.; Di Stefano, P.C.F.; Henry, S.; Kraus, H.; Lynch, A.; Tsybulskyi, V.; Verdier, M.A. Studies of concentration dependences in the luminescence of Ti-doped Al_2O_3. *J. Appl. Phys.* **2011**, *109*, 053116. [CrossRef]

26. Pallotti, D.K.; Passoni, L.; Maddalena, P.; Di Fonzo, F.; Lettieri, S. Photoluminescence mechanisms in anatase and rutile TiO_2. *J. Phys. Chem. C* **2017**, *121*, 9011–9021. [CrossRef]

27. Norrbo, I.; Gluchowski, P.; Hyppanen, I.; Laihinen, T.; Laukkanen, P.; Makela, J.; Lastusaari, M. Mechanisms of tenebrescence and persistent luminescence in synthetic hackmanite $Na_8Al_6Si_6O_{24}(Cl,S)_2$. *ACS Appl. Mater. Interfaces* **2016**, *8*, 11592–11602. [CrossRef]

28. Andrade LH, C.; Lima, S.M.; Novatski, A.; Neto, A.M.; Bento, A.C.; Baesso, M.L.; Boulon, G. Spectroscopic assignments of Ti^{3+} and Ti^{4+} in titanium-doped OH^- free low-silica calcium aluminosilicate glass and role of structural defects on the observed long lifetime and high fluorescence of Ti^{3+} ions. *Phys. Rev. B* **2008**, *78*, 224202. [CrossRef]

29. Gorobets, B.S.; Rogojine, A.A. *Luminescent Spectra of Minerals: Reference-Book*; All-Russia Institute of Mineral Resources (VIMS): Moscow, Russia, 2002; 302p.

30. Taher, M.A.; Asadollahzadeh, H.; Fazelirad, H. Determination of trace amounts of iron by a simple fluorescence quenching method. *Anal. Methods* **2015**, *7*, 6726–6731. [CrossRef]

31. Al-kady, A.S.; Gaber, M.; Hussein, M.M.; Ebeid, E.Z.M. Structural and fluorescence quenching characterization of hematite nanoparticles. *Spectrochim. Acta Part A Mol. Biomol. Spectrosc.* **2011**, *83*, 398–405. [CrossRef]

32. Amthauer, G.; Rossman, G.R. Mixed valence of iron in minerals with cation clusters. *Phys. Chem. Miner.* **1984**, *11*, 37–51. [CrossRef]

33. Fritsch, E.; Waychunas, G.A. *Gemstones. M. Robbins, Fluorescence*; Geoscience Press: Phoenix, AZ, USA, 1994; pp. 163–165.

34. Macke, A.J.H. Luminescence and energy transfer in the ordered perovskite system $La_2MgSn_{1-x}Ti_xO_6$. *Phys. Status Solidi* **1977**, *39*, 117–123. [CrossRef]

35. Macke, A.J.H. Investigations on the luminescence of titanium-activated stannates and zirconates. *J. Solid State Chem.* **1976**, *18*, 337–346. [CrossRef]

36. Wu, Q.; Hu, Z. Na_2TiGeO_5—A self-light-emitting phosphor with the stable structure and tunable emission resulted from Cr^{3+}-doped for FEDs. *J. Am. Ceram. Soc.* **2019**, *102*, 2727–2736.

37. Takahashi, Y.; Masai, h.; Fujiwara, T.; Kitamura, K.; Inoue, S. Afterglow in synthetic bazirite, $BaZrSi_3O_9$. *J. Ceram. Soc. Jpn.* **2008**, *116*, 357–360. [CrossRef]

38. Smith, A.L. Some new complex silicate phosphors containing calcium, magnesium, and beryllium. *J. Electrochem. Soc.* **1949**, *96*, 287. [CrossRef]

39. Evans, B.D.; Pogatshnik, G.J.; Chen, Y. Optical properties of lattice defects in α-Al_2O_3. *Nucl. Instrum. Methods Phys. Res. Sect. B: Beam Interact. Mater. At.* **1994**, *91*, 258–262. [CrossRef]

40. Bausa, L.E.; Vergara, I.; Jaque, F.; Sole, J.G. Ultraviolet laser excited luminescence of Ti-sapphire. *J. Phys. Condens. Matter* **1990**, *2*, 9919. [CrossRef]

41. Marques, C.; Santos, L.; Falcao, A.N.; Silva, R.C.; Alves, E. Luminescence studies in colour centres produced in natural topaz. *J. Lumin.* **2000**, *87*, 583–585. [CrossRef]

42. Iida, Y.; Sawamura, K.; Iwasaki, K.; Nakanishi, T.; Iwakura, F.; Nakajima, Y.; Yasumori, A. Persistent Luminescence Properties of Ti^{4+}-doped $K_2ZrSi_3O_9$ Wadeite. *Sens. Mater.* **2020**, *32*, 1427–1433. [CrossRef]

43. Moon, C.; Nishi, M.; Miura, K.; Hirao, K. Blue long-lasting phosphorescence of Ti-doped $BaZrO_3$ perovskites. *J. Lumin.* **2009**, *129*, 817–819. [CrossRef]

44. Cavignac, T.; Jobic, S.; Latouche, C. Modeling Luminescence Spectrum of $BaZrO_3$: Ti Including Vibronic Coupling from First Principles Calculations. *J. Chem. Theory Comput.* **2022**, *18*, 7714–7721. [CrossRef]

45. Konijnendijk, W.L. Luminescence of $BaSnSi_3O_9$: Ti^{4+} compared to $BaZrSi_3O_9$: Ti^{4+}. *Inorg. Nucl. Chem. Lett.* **1981**, *17*, 129–132. [CrossRef]

46. Zeng, G.; Dong, Q.; Bao, W. Preparation and Photoluminescence Properties of Ti-Doped Lu_2O_3 Powder. *J. Appl. Spectrosc.* **2016**, *83*, 460–465. [CrossRef]

47. Kawano, T.; Yamane, H. Synthesis, crystal structure analysis, and photoluminescence of Ti^{4+}-doped $Mg_5SnB_2O_{10}$. *Chem. Mater.* **2010**, *22*, 5937–5944. [CrossRef]

48. Konijnendijk, W.L.; Blasse, G. On the luminescence of Ti^{4+} in $Mg_5SnB_2O_{10}$ and $Mg_3ZrB_2O_8$. *Mater. Chem. Phys.* **1985**, *12*, 591–599. [CrossRef]

49. Cong, Y.; Li, B.; Yue, S.; Fan, D.; Wang, X.J. Effect of oxygen vacancy on phase transition and photoluminescence properties of nanocrystalline zirconia synthesized by the one-pot reaction. *J. Phys. Chem. C* **2009**, *113*, 13974–13978. [CrossRef]

50. Jochum, K.P.; Weis, U.; Stoll, B.; Kuzmin, D.; Yang, Q.; Raczek, I.; Enzweiler, J. Determination of reference values for NIST SRM 610–617 glasses following ISO guidelines. *Geostand. Geoanalytical Res.* **2011**, *35*, 397–429. [CrossRef]

51. Van Achterbergh, E.; Ryan, C.G.; Griffin, W.L. Glitter: On-line interactive data reduction for the laser ablation inductively coupled plasma mass spectrometry microprobe. In Proceedings of the Ninth Annual VM Goldschmidt Conference, Cambridge, MA, USA, 22–27 August 1999; p. 7215.

52. Sun, R.; Ooi, Y.K.; Dickens, P.T.; Lynn, K.G.; Scarpulla, M.A. On the origin of red luminescence from iron-doped β-Ga_2O_3 bulk crystals. *Appl. Phys. Lett.* **2020**, *117*, 052101. [CrossRef]

53. Gaillou, E.; Fritsch, E.; Massuyeau, F. Luminescence of gem opals: A review of intrinsic an extrinsic emission. *Aust. Gemmol.* **2012**, *24*, 365–373.

54. Gaft, M.; Reisfeld, R.; Panczer, G. *Modern Luminescence Spectroscopy of Minerals and Materials*; Springer: Berlin/Heidelberg, Germany, 2015; 606p.

55. Curtice, R.E.; Scott, A.B. The luminescence of thallium (I) halo complexes. *Inorg. Chem.* **1964**, *3*, 1383–1387. [CrossRef]

56. Ogorodnikov, I.N.; Pustovarov, V.A.; Puzikov, V.M.; Salo, V.I.; Voronov, A.P. A luminescence and absorption spectroscopy study of KH_2PO_4 crystals doped with Tl^+ ions. *Opt. Mater.* **2012**, *34*, 1522–1528. [CrossRef]

57. Kirk, R.D. Role of sulfur in the luminescence and coloration of some aluminosilicates. *J. Electrochem. Soc.* **1954**, *101*, 461. [CrossRef]

58. Stoliaroff, A.; Schira, R.; Blumentritt, F.; Fritsch, E.; Jobic, S.; Latouche, C. Point Defects Modeling Explains Multiple Sulfur Species in Sulfur-Doped $Na_4(Al_3Si_3O_{12})Cl$ Sodalite. *J. Phys. Chem. C* **2021**, *125*, 16674–16680. [CrossRef]

59. Folkerts, H.F.; Blasse, G. Two types of luminescence from Pb^{2+} in alkaline-earth carbonates with the aragonite structure. *J. Phys. Chem. Solids* **1996**, *57*, 303–306. [CrossRef]

60. Lin, J.; Su, Q. Luminescence of Pb^{2+} and energy transfer from Pb^{2+} to rare earth ions in silicate oxyapatites. *Phys. Status Solidi* **1996**, *196*, 261–267. [CrossRef]

61. Folkerts, H.F.; Blasse, G. Luminescence of Pb^{2+} in several calcium borates. *J. Mater. Chem.* **1995**, *5*, 273–276. [CrossRef]

62. Folkerts, H.F.; Hamstra, M.A.; Blasse, G. The luminescence of Pb^{2+} in alkaline earth sulfates. *Chem. Phys. Lett.* **1995**, *246*, 135–138. [CrossRef]

63. Asano, S.; Yamashita, N. Effet du champ magnétique sur la luminescence de l'ion Pb^{2+} dans les luminophores CaO, CaS, CaSe et MgS. *Phys. Status Solidi* **1981**, *108*, 549–558. [CrossRef]

64. Jary, V.; Nikl, M.; Mihokova, E.; Bohacek, P.; Trunda, B.; Polak, K.; Studnicka, V.; Mucka, V. Photoluminescence of Pb^{2+}-doped $SrHfO_3$. *Radiat. Meas.* **2010**, *45*, 406–408. [CrossRef]

65. Tsuboi, T. Temporal Evolution of Luminescence by Pb^{2+}-Doped KBr and KCl Phosphors. *Electrochem. Solid-State Lett.* **2000**, *3*, 200. [CrossRef]

66. Folkerts, H.F.; Blasse, G. Luminescence of Pb^{2+} in $SrTiO_3$. *Chem. Mater.* **1994**, *6*, 969–972. [CrossRef]

67. Skuja, L. Optically active oxygen-deficiency-related centers in amorphous silicon dioxide. *J. NON-Cryst. Solids* **1998**, *239*, 16–48. [CrossRef]

68. Yu, D.P.; Hang, Q.L.; Ding, Y.; Zhang, Z.G.; Bai, Z.G.; Wang, J.J.; Zou, Y.H.; Qian, Q.; Xiong, G.C.; Feng, S.Q. Amorphous silica nanowires: Intensive blue light emitters. *Appl. Phys. Lett.* **1998**, *73*, 3076–3078. [CrossRef]

69. Nassau, K. *Gems Made by Man*, 1st ed.; Chilton Book Co.: Radnor, PA, USA, 1980; p. 364.

70. Gauthier, J.P. Observation directe par microscopie électronique à transmission de diverses variétés d'opale. II. Opale synthétique. *J. De Microsc. Et De Spectrosc. Electron.* **1986**, *11*, 37–52.

71. Mason, B. *Principle of Geochemistry*, 3rd ed.; John Wiley and Sons: New York, NY, USA, 1952; p. 276.

72. Waychunas, G.A. Synchrotron radiation XANES spectroscopy of Ti in minerals; effects of Ti bonding distances, Ti valence, and site geometry on absorption edge structure. *Am. Mineral.* **1987**, *72*, 89–101.

73. Morrison, G.; Christian, M.S.; Besmann, T.M.; Zur Loye, H.C. Flux Growth of Uranyl Titanates: Rare Examples of TiO_4 tetrahedra and TiO_5 square bipyramids. *J. Phys. Chem. A* **2020**, *124*, 9487–9495. [CrossRef]

74. Jiang, N.; Su, D.; Spence, J.C.H. Determination of Ti coordination from pre-edge peaks in Ti K-edge XANES. *Phys. Rev. B* **2007**, *76*, 214117. [CrossRef]

75. Ichihashi, Y.; Yamashita, H.; Anpo, M.; Souma, Y.; Matsumura, Y. Photoluminescence properties of tetrahedral titanium oxide species in zeolitic materials. *Catal. Lett.* **1998**, *53*, 107–109. [CrossRef]

76. Nichols, E.L. The luminescence of titanium oxide. *Phys. Rev.* **1923**, *22*, 420. [CrossRef]

77. Satoh, Y.; Takemoto, M. Charge transfer-type fluorescence of Ti-doped $Ca_{14}Al_{10}Zn_6O_{35}$. *J. Lumin.* **2017**, *185*, 141–144. [CrossRef]

78. Keil, K.; Fuchs, L.H. Hibonite [$Ca_2(Al,Ti)_{24}O_{38}$] from the Leoville and Allende chondritic meteorites. *Earth Planet. Sci. Lett.* **1971**, *12*, 184–190. [CrossRef]

79. Hall, M.R.; Ribbe, P.H. An electron microprobe study of luminescence centers in cassiterite. *Am. Mineral. J. Earth Planet. Mater.* **1971**, *56*, 31–45.

80. Bloise, A.; Pingitore, V.; Miriello, D.; Apollaro, C.; Armentano, D.; Barrese, E.; Oliva, A. Flux growth and characterization of Ti-and Ni-doped enstatite single crystals. *J. Cryst. Growth* **2011**, *329*, 86–91. [CrossRef]

81. Zhang, S.; Zhang, P.; Liu, X.; Yang, Z.; Huang, Y.; Seo, H.J. Synthesis, structure, and luminescence of Eu^{3+}-activated $La_4Ti_3O_{12}$ nanoparticles with layered perovskite structure. *J. Am. Ceram. Soc.* **2019**, *102*, 1784–1793. [CrossRef]

82. Freitas, G.F.G.; Nasar, R.S.; Cerqueira, M.; Melo, M.; Longo, E.; Varela, J.A. Luminescence in semi-crystalline zirconium titanate doped with lanthanum. *Mater. Sci. Eng. A* **2006**, *434*, 19–22. [CrossRef]

83. Blasse, G.; Dirksen, G.J. The luminescence of barium titanium phosphate, $BaTi(PO_4)_2$. *Chem. Phys. Lett.* **1979**, *62*, 19–20. [CrossRef]

84. Li, Y.; Zhou, Y.; Xiao, J.; Yang, D.; Dai, L.; Yang, Y.; Zhao, L. A rare-earth-free self-activated phosphor: Li_2TiSiO_5 with TiO_5 square pyramids. *N. J. Chem.* **2020**, *44*, 5828–5833. [CrossRef]

85. Ding, J.; Li, Y.; Wu, Q.; Long, Q.; Wang, Y.; Wang, Y. A novel self-activated white-light-emitting phosphor of Na_2TiSiO_5 with two Ti sites of TiO_5 and TiO_6. *RSC Adv.* **2016**, *6*, 8605–8611. [CrossRef]

86. Takahashi, Y.; Kitamura, K.; Iyi, N.; Inoue, S. Visible orange photoluminescence in a barium titanosilicate $BaTiSi_2O_7$. *Appl. Phys. Lett.* **2006**, *88*, 151903. [CrossRef]

87. De Haart, L.G.J.; De Vries, A.J.; Blasse, G. On the photoluminescence of semiconducting titanates applied in photoelectrochemical cells. *J. Solid State Chem.* **1985**, *59*, 291–300. [CrossRef]

88. Huang, Y.; Tsuboi, T.; Seo, H.J. A high efficient $Ba_2TiP_2O_9$ phosphor for X-ray and UV excitation. *Ceram. Int.* **2013**, *39*, 861–864. [CrossRef]

89. Bouma, B.; Blasse, G. Dependence of luminescence of titanates on their crystal structure. *J. Phys. Chem. Solids* **1995**, *56*, 261–265. [CrossRef]

90. De Figueiredo, A.T.; Longo, V.M.; de Lazaro, S.; Mastelaro, V.R.; De Vicente, F.S.; Hernandes, A.C.; Longo, E. Blue-green and red photoluminescence in $CaTiO_3$: Sm. *J. Lumin.* **2007**, *126*, 403–407. [CrossRef]

91. Ma, Q.; Zhang, A.; Lue, M.; Zhou, Y.; Qiu, Z.; Zhou, G. Novel class of aeschynite structure $LaNbTiO_6$-based orange-red phosphors via a modified combustion approach. *J. Phys. Chem. B* **2007**, *111*, 12693–12699. [CrossRef]

92. Lin, Y.; Nan, C.W.; Wang, J.; He, H.; Zhai, J.; Jiang, L. Photoluminescence of nanosized $Na_{0.5}Bi_{0.5}TiO_3$ synthesized by a sol–gel process. *Mater. Lett.* **2004**, *58*, 829–832. [CrossRef]

93. Parsons, I.; Steele, D.A.; Lee, M.R.; Magee, C.W. Titanium as a cathodoluminescence activator in alkali feldspars. *Am. Mineral.* **2008**, *93*, 875–879. [CrossRef]

94. Cathelineau, T. Catapleiite from Mont Saint-Hilaire, Québec, Canada. *J. Gemmol.* **2020**, *37*, 237–239. [CrossRef]

95. Silva Santos, H.; Norrbo, I.; Laihinen, T.; Sinkkonen, J.; Mäkilä, E.; MCarvalho, J.; Lastusaari, M. Synthesis and Features of Luminescent Bromo-and Iodohectorite Nanoclay Materials. *Appl. Sci.* **2017**, *7*, 1243. [CrossRef]

96. Yamashita, T.; Ueda, K. Blue photoluminescence in Ti-doped alkaline-earth stannates. *J. Solid State Chem.* **2007**, *180*, 1410–1413. [CrossRef]

97. Xia, M.; Zhang, Y.; Li, M.; Zhong, Y.; Gu, S.; Zhou, N.; Zhou, Z. High thermal stability and blue-violet emitting phosphor $CaYAlO_4$: Ti^{4+} with enhanced emission by Ca^{2+} vacancies. *J. Rare Earths* **2020**, *38*, 227–233. [CrossRef]

98. Wong, W.C.; Danger, T.; Huber, G.; Petermann, K. Spectroscopy and excited-state absorption of Ti^{4+}: $Li_4Ge_5O_{12}$ and Ti^{4+}: Y_2SiO_5. *J. Lumin.* **1997**, *72*, 208–210. [CrossRef]

99. Lin, C.M.; Lai, Y.-S.; Chen, J.S. Photoluminescence behavior of Ti-doped Zn_2SiO_4 thin film phosphors. *ECS Trans.* **2006**, *1*, 1. [CrossRef]

100. Haldar, P.K.; Dey, S.; Mukhopadhyay, S.; Mukhopahyay, S.; Parya, T.K. Structural and optical properties of Ti^{4+} doped sintered $ZnAl_2O_4$ ceramics. *Interceram-Int. Ceram. Rev.* **2014**, *63*, 382–385. [CrossRef]

101. Alajerami, Y.S.M.; Hashim, S.; Hassan, W.M.S.W.; Ramli, A. The effect of titanium oxide on the optical properties of lithium potassium borate glass. *J. Mol. Struct.* **2012**, *1026*, 159–167. [CrossRef]

102. Fischer, K. Verfeinerung der Kristallstruktur von Benitoit BaTi [Si309]. *Z. Für Krist.-Cryst. Mater.* **1969**, *129*, 222–243. [CrossRef]

103. Sandomirskii, P.A.; Simonov, M.A.; Belov, N.V. Crystal structure of baratovite, $KLi_3Ca_7Ti_2(Si_6O_{18})_2F_2$. In *Doklady Akademii Nauk*; Russian Academy of Sciences: Moscow, Russia, 1976; pp. 615–618.

104. Kato, T.; Murakami, N. The crystal structure of katayamalite. *Mineral. J.* **1985**, *12*, 206–217. [CrossRef]

105. Sundberg, M.R.; Lehtinen, M.; Kivekas, R. Refinement of the crystal structure of ramsayite (lorenzenite). *Am. Mineral.* **1987**, *72*, 173–177.

106. Speer, J.A.; Gibbs, G.V. The crystal structure of synthetic titanite, $CaTiOSiO_4$, and the domain textures of natural titanites. *Am. Mineral.* **1976**, *61*, 238–247.

107. Merlino, S.; Pasero, M.; Artioli, G.; Khomyakov, A.P. Penkvilksite, a new kind of silicate structure: OD character, X-ray single-crystal (1 M), and powder Rietveld (2O) refinements of two MDO polytypes. *Am. Mineral.* **1994**, *79*, 1185–1193.

108. Horn, M.S.C.F.; Schwebdtfeger, C.F.; Meagher, E.P. Refinement of the structure of anatase at several temperatures. *Z. Krist.-Cryst. Mater.* **1972**, *136*, 273–281.

109. Monarumit, N.; Wongkokua, W.; Satitkune, S. Oxidation state of Ti atoms and Ti-O bond length on natural sapphire gem-materials probed by X-ray absorption spectroscopy. In *Key Engineering Materials*; Trans Tech Publications Ltd.: Wollerau, Switzerland, 2017; pp. 585–589.

110. Sasaki, S.; Prewitt, C.T.; Bass, J.D.; Schulze, W.A. Orthorhombic perovskite $CaTiO_3$ and $CdTiO_3$: Structure and space group. *Acta Crystallogr. Sect. C: Cryst. Struct. Commun.* **1987**, *43*, 1668–1674. [CrossRef]

111. Yakubovich, O.V.; Kireev, V.V. Refinement of the crystal structure of $Na_2Ti_3O_7$. *Crystallogr. Rep.* **2003**, *48*, 24–28. [CrossRef]

112. Ziadi, A.; Thiele, G.; Elouadi, B. The crystal structure of Li_2TiSiO_5. *J. Solid State Chem.* **1994**, *109*, 112–115. [CrossRef]

113. Nyman, H.; O'Keeffe, M.; Bovin, J.O. Sodium titanium silicate, Na_2TiSiO_5. *Acta Crystallogr. Sect. B: Struct. Crystallogr. Cryst. Chem.* **1978**, *34*, 905–906. [CrossRef]

114. Longo, J.M.; Kierkegaard, P. The crystal structure of NbOPO$_4$. *Acta Chem. Scand.* **1966**, *20*, 72–78. [CrossRef]

115. Robertson, A.; Fletcher, J.G.; Skakle, J.M.S.; West, A.R. Synthesis of LiTiPO$_5$ and LiTiAsO$_5$ with the α-Fe$_2$PO$_5$ structure. *J. Solid State Chem.* **1994**, *109*, 53–59. [CrossRef]

116. Culbertson, C.M.; Flak, A.T.; Yatskin, M.; Cheong, P.H.Y.; Can, D.P.; Dolgos, M.R. Neutron total scattering studies of group ii titanates (ATiO$_3$, A^{2+} = Mg, Ca, Sr, Ba). *Sci. Rep.* **2020**, *10*, 1–10. [CrossRef]

117. Tordjman, P.I.; Masse, E.; Guitel, J.C. Structure cristalline du monophosphate KTiPO$_5$. *Z. Krist.* **1974**, *139*, 103–115. [CrossRef]

118. Golobič, A.; Škapin, S.D.; Suvorov, D.; Meden, A. Solving structural problems of ceramic materials. *Croat. Chem. Acta* **2004**, *77*, 435–446.

119. Yoneda, Y.; Noguchi, Y. Nanoscale structural analysis of Bi$_{0.5}$Na$_{0.5}$TiO$_3$. *Jpn. J. Appl. Phys.* **2020**, *59*, SPPA01. [CrossRef]